PHYSICAL REVIEW A **73**, 012706 (2006)

Measurement of the photoionization cross section of the $(2p)^5(3p)\ ^3D_3$ state of neon

B. J. Claessens,[1] J. P. Ashmore,[2] R. T. Sang,[2] W. R. MacGillivray,[2,*] H. C. W. Beijerinck,[1] and E. J. D. Vredenbregt[1,†]
[1]*Department of Applied Physics, Eindhoven University of Technology, P.O. Box 513, 5600 MB Eindhoven, The Netherlands*
[2]*Centre for Quantum Dynamics, School of Science, Griffith University, Nathan QLD 4111, Australia*
()

We report a new measurement of the photoionization cross section for the $(2p)^5(3p)\ ^3D_3$ state of neon at the wavelengths of 351 and 364 nm. These data were obtained by monitoring the decay of the fluorescence of atoms trapped in a magneto-optical atom trap under the presence of a photoionizing laser, a technique developed by Dinneen *et al.* [Opt. Lett. **17**, 1706 (1992)]. We obtain absolute photoionization cross sections of $2.05\pm0.25\times10^{-18}$ cm^2 at $\lambda=351$ nm and $2.15\pm0.25\times10^{-18}$ cm^2 at $\lambda=364$ nm, an improvement in accuracy of a factor of 4 over previously published values. These new values are not consistent with published theoretical data.

()

I. INTRODUCTION

The process of photoionization plays an important role in applied plasmas such as gas lasers or discharge lamps, and also as a technique for producing ionized matter for scientific study. Recently, for instance, it has become possible to study a virtually unexplored field in plasma physics experimentally through the production of a so-called ultracold plasma [1] by near-threshold photoionization of a sample of neutral atoms trapped in a magneto-optical trap (MOT). Such ultracold plasmas have ion temperatures around 1 mK and electron temperatures as low as 10 K at a density of about 10^9 cm^{-3}, at which point the electrostatic interaction energy between nearest neighbors becomes comparable to the kinetic energy. The plasma is then close to entering the strongly coupled regime where standard classical plasma physics assumptions may become invalid [2,3].

Photoionization cross sections furthermore provide fundamental tests of atomic structure calculations [4–19]. Here, as is often the case, alkali-metal atoms and rare gas atoms are of particular importance as relatively simple test subjects. For ionization out of the ground state, absolute cross sections have been determined with great precision (uncertainty 1–3 %) over a wide range of photon energies of up to 4000 eV by using synchrotron radiation [5–7]. For excited states, ionization close to threshold has been studied using discharge and laser-excited atomic beams [8–13] and, only for alkali-metal atoms, also using atom traps [16–19]. In the latter case, absolute values could be determined with an accuracy down to 10%.

The atom trap technique was pioneered by Dinneen *et al.* [16] and later applied by several other groups [17–19], with all experiments focusing exclusively on rubidium. Here we follow this lead to obtain absolute and precise measurements of the photoionization cross section of the excited $(2p)^5(3p)\ ^3D_3$ state of neon for two different ionization wavelengths. While much has been learned about photoionization out of this and closely related states from, e.g., photoelectron spectra [10], electron angular distributions [11], and autoionization widths [12,13,15], so far the absolute value of the corresponding cross sections has only been known with a relative accuracy of 50% [10,11]. In this paper we present an independent and direct measurement based on studying the effect of an ionizing laser on the decay dynamics of laser-excited neon atoms trapped in a magneto-optical trap. The technique used here employs only relative measurements of atom numbers, which allowed the relative precision to be increased by a factor of 4 over the measurements of Siegel *et al.* [11]. At the time, these authors necessarily had to rely on data on collisional ionization processes to obtain an absolute value of their atom flux, which restricted the achieved accuracy.

This paper is organized as follows: Sec. II describes the experimental setup and the characteristics of the photoionization laser; Sec. III presents the experimental results and the corresponding analysis; Sec. IV discusses the results and the corresponding uncertainties and compares our measured values with previous work.

II. EXPERIMENTAL SETUP

Metastable neon atoms are trapped in a MOT which is loaded from a bright atomic beam as described in Refs. [20,21]. The atomic beam can produce approximately 2×10^{10} atoms per second traveling at 100 m/s. These atoms are slowed down further in a second Zeeman slower and trapped in a MOT. The magnetic field gradient of the MOT is about 10 G/cm, and the detuning of the trapping laser was set at -0.5Γ with $\Gamma=(2\pi)8.2$ MHz the natural width of the atomic transition.

The laser light used for all laser cooling stages of both the atomic beam and the MOT was generated with a frequency stabilized Coherent 899 ring dye laser. This laser produces 700 mW of laser light at a wavelength of 640.224 nm, resonant with the closed Ne $(2p)^5(3s)\ ^3P_2\rightarrow(2p)^5(3p)\ ^3D_3$ optical transition. The laser light for the MOT beams was spatially filtered through a fiber and expanded. The MOT beams

*Present address: Faculty of Science, University of Southern Queensland, Toowoomba QLD 4350, Australia.
†Electronic address: e.j.d.vredenbregt@tue.nl

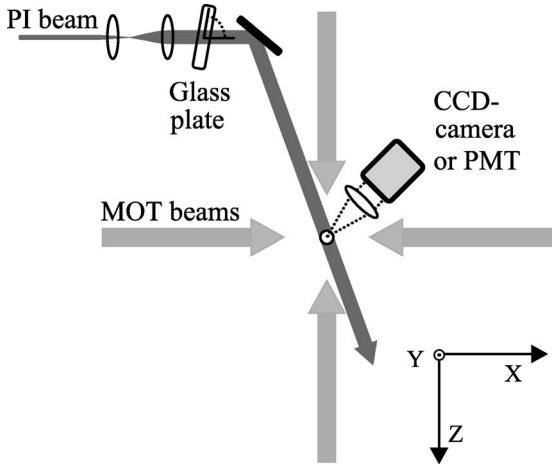

FIG. 1. Schematic drawing of the MOT and the uv laser beam. Depicted in the figure is the telescope used for expanding the PI beam and the glass plate used for moving the PI beam with respect to the atom cloud.

have a Gaussian beam profile with a $1/\sqrt{e}$ intensity radius of 1.5 ± 0.1 mm. The combined intensity of all MOT beams was typically 16 mW/cm^2.

The spatial profile of the fluorescence emitted by the MOT was imaged with a charge-coupled-device (CCD) camera and had a profile that could be fitted well with a Gaussian distribution. The $1/\sqrt{e}$ radius of the MOT fluorescence in the x (s_x) and z (s_z) (see Fig. 1) direction was measured to be 80 ± 20 μm. The intensity of the MOT beams was stabilized to better than 10^{-2} using a electronic controller connected to the modulation input of an AOM driver. The stabilization was built such that we could switch between two stabilized intensities within 400 μs.

The uv light for photoionization (PI beam) was produced with a Coherent Innova 90-5 argon-ion laser which we used in two different modes: (i) a dual wavelength mode or "mixed mode," in which the laser generates a maximum of 86.5 mW of 364-nm light and 53.5 mW of 351-nm light simultaneously, and (ii) a "nonmixed mode" in which the laser generates a maximum of 80 mW at 351 nm only.

Both these wavelengths generated by the laser are greater than 290 nm, the maximum wavelength for photoionization from the $(2p)^5(3s)\ ^3P_2$ state. This ensures that photoionization only occurs from the $(2p)^5(3p)\ ^3D_3$ state. The Gaussian PI beam was expanded to a $1/\sqrt{e}$ intensity radius of 450 ± 20 μm in the x direction and 530 ± 20 μm in the y direction at the position of the MOT (see Fig. 1). The beam was passed through an antireflection coated glass plate, enabling small, controlled horizontal and vertical movements of the PI beam relative to the atom cloud, and then sent through a vacuum window into the trap under a small angle with the z direction. The transmission of the vacuum window was measured to be 0.73 ± 0.02 at 351 nm and 0.80 ± 0.02 at 364 nm.

Relevant information was obtained via the measurement of the decay fluorescence using a Pulnix TM 1300 CCD camera. The camera measured total fluorescence power emitted by the trapped atoms at a rate of 10 frames/s. The fluorescence of the atoms could also be detected with an EMI 9862K photomultiplier tube (PMT). This was used to measure fast ($\leqslant$400 μs) changes in fluorescence power, resulting from a sudden change in MOT laser intensity. Both the CCD camera and the photomultiplier tube were only used for relative measurements so that calibration for absolute detection efficiency was not necessary.

A schematic representation of the MOT setup and the PI beam is given in Fig. 1.

III. MEASUREMENT OF THE PHOTOIONIZATION CROSS SECTION

A. Linear loss rate

The rate equation that describes the time evolution of the number of trapped atoms N_t in the MOT with the presence of the PI beam is

$$\frac{dN_t}{dt} = R_L - N_t(\Gamma_{BG} + \Gamma_{PI}) - \beta \int n(\mathbf{r},t)^2 d\mathbf{r}, \qquad (1)$$

where R_L is the loading rate (determined by the beam flux and the capture efficiency of the MOT) and Γ_{BG} is the decay rate due to density-independent losses such as background gas collisions (the pressure in the trap chamber during operation is approximately 1.6×10^{-9} mbar). The rate constant β describes the density-dependent losses and $n(\mathbf{r},t)$ is the atomic density distribution of the trapped atoms. Finally, Γ_{PI} is the decay rate due to photoionization from which the photoionization cross section can be determined as we show in Sec. III B.

One aspect that makes photoionization experiments with metastable atoms different compared to similar experiments with alkali atoms is that the steady-state number in the MOT is mainly determined by two body losses [21]. A consequence of this is that it is very difficult to measure Γ_{PI} by studying the effect of the photoionization laser on the steady-state number of atoms in the MOT. Only its effect on the fill rate or on the decay rate of the MOT, and then only at low densities can be used. Here the dynamics are determined by linear losses, i.e., density independent losses. In this experiment we chose to study the decay dynamics when the atomic beam is switched off ($R_L=0$) since then the results do not suffer from fluctuations in the beam flux.

In our trap the spatial distribution is to a good approximation independent of the number of atoms [21], i.e., $n(\mathbf{r},t) = n(\mathbf{r})g(t)$ so that the solution to Eq. (1) (with $R_L=0$) can be written as

$$N_t(t) = \frac{N_t(0)\exp(-tR)}{1+[\beta N_t(0)/V_{eff}][1-\exp(-tR)]}, \qquad (2)$$

where $V_{eff}=(2\pi)^{3/2}s_x s_y s_z$ is the effective trap volume [21] and $R=\Gamma_{BG}+\Gamma_{PI}$ is the total decay rate. Figure 2 shows two typical experimental decay curves fitted with Eq. (2), with and without the presence of the photoionizing laser. Fits to the data such as these enable R to be determined. For both curves the initial part of the decay is dominated by two-body losses. The effect of linear losses becomes visible at lower atom numbers, and therefore lower atomic densities.

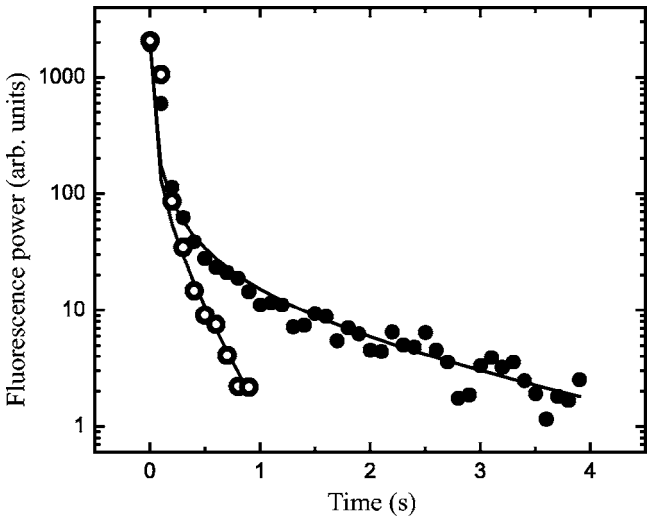

FIG. 2. Fluorescence power from the atoms trapped in the MOT as a function of time after loading is stopped, without (filled circles) and with (open circles) the presence of the PI beam. The solid lines are fits to Eq. (2).

B. Loss rate vs uv intensity

The linear decay rate Γ_{PI} due to photoionization by a monochromatic light source with frequency ν can be written as

$$\Gamma_{PI} = \frac{I_{PI} f \sigma}{h\nu}, \tag{3}$$

where I_{PI} is the average photoionizing laser intensity incident on the $^3D_3$ atoms in the MOT, h is Planck's constant and σ is the photoionization cross section at frequency ν [16]. The decay rate is proportional to the excited state fraction f, i.e., the fraction of atoms in the excited $^3D_3$ state, since only these atoms can be ionized with the uv laser as discussed in Sec. II. As the size of the atom cloud is much smaller than the diameter of the trapping beams, f is constant over the trapping region. Note that Eq. (3) is only valid when I_{PI} is far from saturation; in the present experiment this is always the case. By measuring R as a function of the average photoionizing laser intensity I_{PI}, a value for $f\sigma$ can be determined.

The value of I_{PI} is determined by the total uv laser power (P_{uv}) and the spatial profile of the photoionizing laser $I(x,y)$, given by

$$I(x,y) = I_0 \exp\left(-\frac{x^2}{2\sigma_x^2}\right)\exp\left(-\frac{y^2}{2\sigma_y^2}\right), \tag{4}$$

with σ_x and σ_y the $1/\sqrt{e}$ radii of the PI beam in the x and y directions and $I_0 = P_{\mathrm{uv}}/(2\pi\sigma_x\sigma_y)$ the peak intensity. Furthermore, the spatial profile of the ($^3D_3$) atoms in the MOT and the alignment of the MOT with respect to the uv laser have to be taken into account. As mentioned in Sec. II we measured the spatial profiles of both the $^3D_3$ atoms and the PI laser by imaging them on a CCD camera and found that both spatial profiles were fitted well with a Gaussian distribution. Assuming that the MOT and the PI beam are well aligned with respect to one another (we will discuss alignment of the MOT and PI beam further in Sec. IV), the average intensity can be found by averaging the spatial profile $I(x,y)$ given by Eq. (4) over the normalized, transverse, spatial distribution $\tilde{n}(x,y)$ of the trapped atoms,

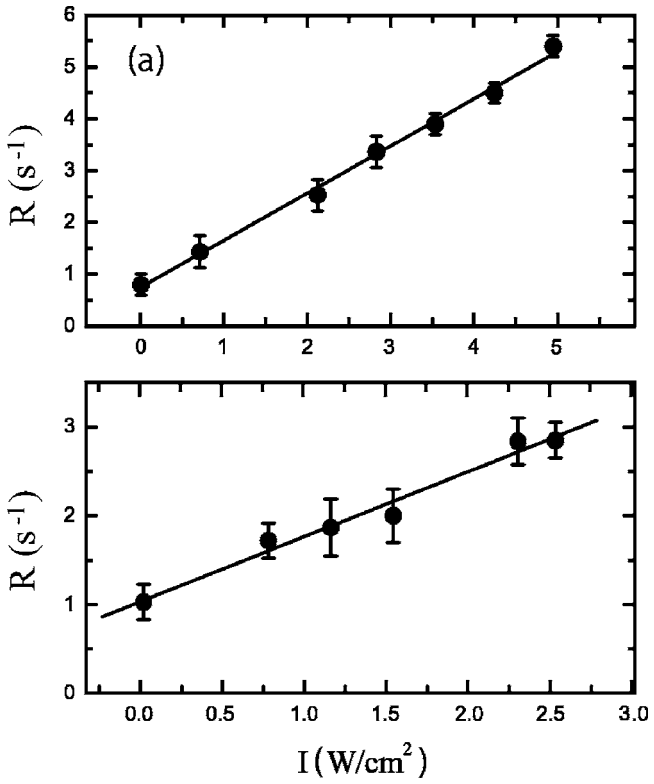

FIG. 3. The upper graph (a) shows the measured linear loss rate as a function of intensity of the mixed-mode PI beam. The lower graph (b) shows the fitted loss rate as a function of intensity of the 351-nm-only PI beam. The solid lines are linear fits to the data.

$$I_{PI} = \int\int I(x,y)\tilde{n}(x,y)dxdy = \frac{I_0\sigma_x\sigma_y}{\sqrt{(\sigma_x^2+s_x^2)(\sigma_y^2+s_y^2)}}, \tag{5}$$

where (as before) s_x and s_y are the $1/\sqrt{e}$ radii in the x and y direction of the spatial profile of the $^3D_3$ atoms. Since the size of the PI beam is much larger than the size of the $^3D_3$ atom distribution, the value of I_{PI}/I_0 is rather insensitive to fluctuations in the size of the $^3D_3$ atom distribution.

Figure 3(a) shows the measured linear loss rate as a function of intensity seen by the atoms when the laser was running in mixed mode (both 351- and 364-nm light). Each data point is a statistical average of at least five measurements. Figure 3(b) shows the measured linear loss rate as a function of intensity seen by the atoms with the laser running in non-mixed mode (351 nm only). Once again, each data point is a statistical average of at least five separate measurements. The linear behavior of the data confirms the assumption of a loss rate constant that varies linearly with the laser intensity. The slope of these curves corresponds to the quantity $f\sigma/h\nu = 0.79 \pm 0.05$ cm^2/J for the 351-nm-only beam, and $f\langle\sigma/h\nu\rangle = 0.83 \pm 0.02$ cm^2/J for the mixed mode uv beam, where $\langle\cdots\rangle$ indicates averaging according to the fractional power of the PI beam at the wavelengths of 364 and 351 nm.

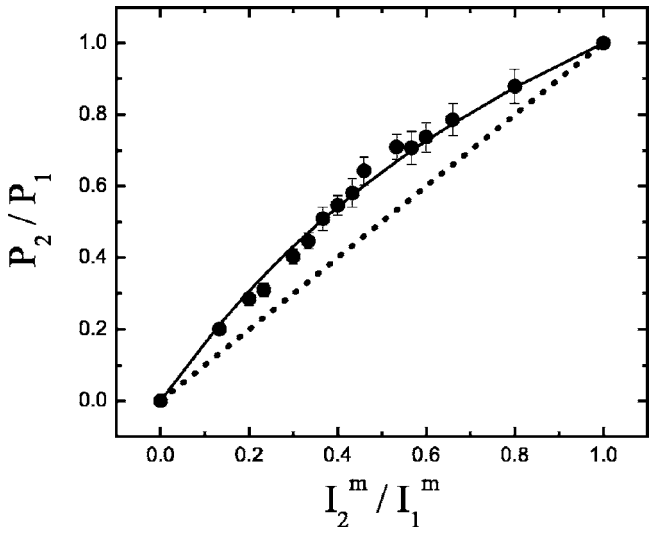

FIG. 4. Measured ratio of fluorescence powers P_2/P_1 as a function of the ratio of intensities I_2^m/I_1^m. Every point is a statistical average over at least eight measurements. The solid line is a fit to the data using Eq. (7). The dotted line represents Eq. (7) for $A=0$.

C. Excited state fraction

To determine σ, the excited state fraction f must be ascertained. In order to overcome cumbersome calculations to determine the excited state fraction [22], we used an empirical expression developed by Townsend *et al.* [23],

$$f=\frac{1}{2}\frac{CS}{1+4\delta^2+CS}. \tag{6}$$

Here, $S=I^m/I_0^m$, where I_0^m is the saturation intensity of the $^3P_2\rightarrow{}^3D_3$ transition, and I^m is the laser intensity of all MOT beams combined. The detuning of the MOT beams δ is expressed in units of Γ, and for this experiment was set to $\delta=-0.5$. The quantity C is a phenomenological factor which lies between the average of the squared Clebsch-Gordan coefficients of all involved transitions and 1. For the $^3P_2\rightarrow{}^3D_3$ transition, the average of the squared Clebsch-Gordan coefficients is 0.46.

The large uncertainty in C and in the effective intensity I^m seen by the atoms, due to laser beam imbalances and alignment uncertainties, makes it necessary to measure the excited state fraction. For this we adopted a modified version of the technique used by Townsend *et al.* [23]. We measured the power P_1 of the fluorescence scattered by the atoms at a certain trap-laser intensity I_1^m, which is proportional to the excited state fraction f_1 at that intensity. We then suddenly changed the intensity and measured the power P_2 of the fluorescence emitted by the atoms with the new intensity I_2^m (Townsend *et al.* applied a rapid change in detuning). The intensity was changed fast enough to make sure the loss in atom number and the movement of the atoms may be neglected.

Figure 4 shows the ratio P_2/P_1 as function of the ratio between the two intensities I_2^m/I_1^m. Our data fits well with the following equation:

$$\frac{f_2}{f_1}=\frac{I_2^m}{I_1^m}\frac{1+A}{1+A(I_2^m/I_1^m)}, \tag{7}$$

derived from Eq. (6). Here, $A=CI_1^m/I_0^m(1+4\delta^2)$ is the only fit parameter. Having determined $A=0.77\pm0.06$ in this way from the data in Fig. 4, we find the excited state fraction at the MOT laser intensity used in the decay experiments (corresponding to $I_2^m/I_1^m=1$) to be 21.7 ± 1.5 %. From Eq. (6) it follows that $f=(1/2)A/(1+A)$ so that uncertainties in the value of the detuning have no influence on this determination.

From the fitted value of A we can extract an estimate for C by inserting the calculated effective intensity I^m of the MOT beams, which serves as a consistency check. This results in a value of 0.4 ± 0.1 for the phenomenological constant C, which is indeed in the expected range. We note that this cannot be regarded as an actual measurement of C since which we did not independently determine the intensity of the trapping light experienced by the atoms.

IV. SOURCES OF UNCERTAINTY AND CONCLUSIONS

Combining the measurements of the linear loss rate $f\sigma$ due to photoionization and the excited state fraction f yields a value of $2.05\pm0.18\times10^{-18}$ cm^2 for σ at 351 nm, and a value of $2.15\pm0.16\times10^{-18}$ cm^2 at 364 nm. The value for the cross section at 351 nm was determined directly from the measurements with the laser in nonmixed mode. The value obtained was then used to extract the cross section at 364 nm from the measurements with the laser in mixed mode. We note that these cross sections correspond to effectively unpolarized atoms, due to the presence of trapping beams with various polarizations. The uncertainties given here correspond only to the statistical standard deviations as determined by the measurements of total loss rate R vs PI intensity I_{PI} and the excited state fraction f (which is the dominant source of the uncertainty).

In our measurements there were also several systematic sources of uncertainty; all of these are related to the precision with which the average intensity I_{PI} is known, estimated to be within 8%. This comes mainly from four contributions: (i) The uncertainty of the transmission through the vacuum window between the point where we measured the power and where the atoms are (2%); (ii) The uncertainty in the power measured with our power meter (5%); (iii) The uncertainty in determining the waists of both the uv laser and the atomic distribution in the MOT. This gives an uncertainty in the determined intensity of 3%; (iv) The alignment of the uv laser with respect to the atom cloud. Special care was taken to make sure that the photoionization beam was aligned with respect to the MOT. Figure 5 shows the effective decay rate as a function of horizontal (a) and vertical (b) displacements of the PI beam with respect to the MOT, displaced via the rotatable glass plate (see Fig. 1). Based on these measurements we conclude that the MOT was within 0.3σ of the $1/\sqrt{e}$ intensity radius σ of the PI beam. This gives an additional uncertainty of 5% for the average intensity.

Taking these various uncertainties into account by adding them quadratically, we conclude that we measured the cross

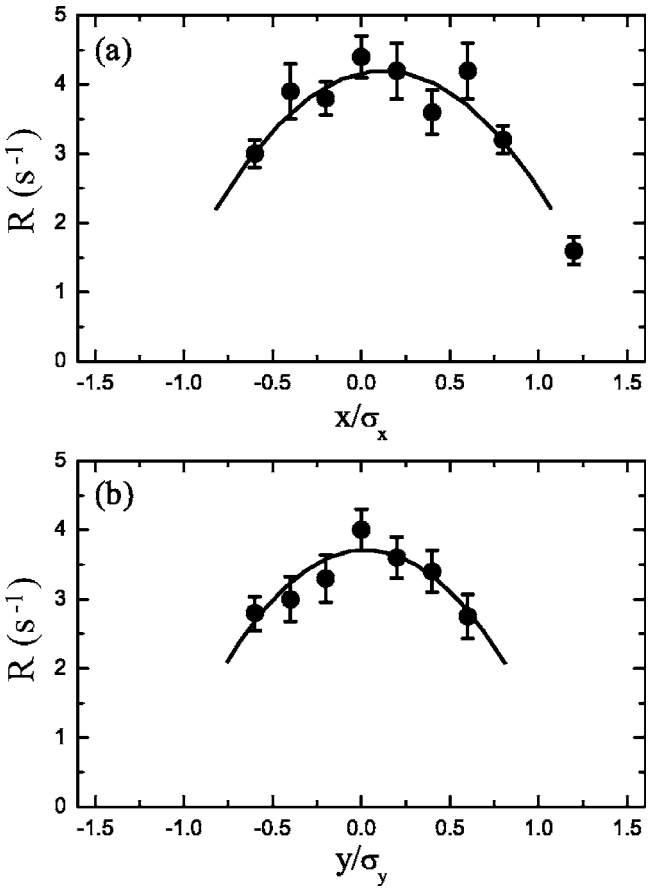

FIG. 5. Linear loss rate as a function of the relative displacement of the PI beam with respect to the atom cloud in (a) the x direction, and (b) the y direction. The curves represent parabolic fits to the data.

section for Ne $^3D_3$ atoms to be $2.05\pm0.25\times10^{-18}$ cm^2 at a wavelength of 351 nm and $2.15\pm0.25\times10^{-18}$ cm^2 at a wavelength of 364 nm. The relative accuracy obtained ($\approx12\%$) is quite comparable to the result of Dinneen *et al.* using rubidium and is dominated by the contribution from the excited state fraction.

When we compare our measurement with previous experimental work done at 351 nm by Siegel *et al.* [11] using an atomic beam, then we find that our measurements are in perfect agreement with their value but a factor of 4 more precise. These authors determined the photoionization cross section at 351 nm to be $(2\pm1)\times10^{-18}$ cm^2 by reference to data on collisional ionization on which their absolute flux of excited state atoms could be calibrated. As the measurements here only rely on relative atom numbers as measured by the fluorescence yield, in principle they can be made arbitrarily more precise by further improvement of the statistical accuracy and elimination of systematical errors.

For neon there do not seem to exist any recent calculations of absolute cross sections for ionization out of the $3p$ state, in contrast to the situation for the metastable $(3s)$ $^3P_{0,2}$ states [14]. To compare the experimental data we have to refer back to somewhat older theoretical values from Duzy and Hyman [24], from Chang [25], and from Chang and Kim [26]. Duzy and Hyman used a central-field approximation for the potential experienced by the outer electron, including a core polarizability that was adjusted semiempirically to generate binding energies that would match experimental data of about 15 excited states. Fine-structure effects were not taken into account. The photoionization cross sections were subsequently calculated from the resulting wave function of the outer electron. In this way, a value of $\approx5\times10^{-18}$ cm^2 for the cross section at 364 nm was obtained. Chang [25] instead applied a Hartree-Fock treatment which included the influence of many-body corrections to the cross section; these, however, turned out to be quite small ($<10\%$) for ionization wavelengths greater than 340 nm. In a subsequent paper therefore Chang and Kim [26] used a single-configuration Hartree-Fock treatment and found $\sigma\approx4.5\times10^{-18}$ cm^2 at 364 nm, with about a 10% smaller value at 351 nm. All these values are beyond the high 3σ border of our data. This suggests that a refinement of the calculations may be in order, for which the current data may serve as a benchmark.

ACKNOWLEDGMENTS

We would like to thank A. Kemper, R. Rumphorst, W. Kemper, H. van Doorn, V. Mogendorff, C. Hawthorn, L. van Moll, J. van de Ven, and R. Gommers for technical and experimental assistance. We also acknowledge useful communications with H. Hotop, and thank Coherent Netherlands B.V. for the loan of the Innova 90 laser used in these experiments. This work was financially supported by the Australian Research Council and the Netherlands Foundation for Fundamental Research on Matter (FOM).

[1] T. C. Killian, S. Kulin, S. D. Bergeson, L. A. Orozco, C. Orzel, and S. L. Rolston, Phys. Rev. Lett. **83**, 4776 (1999).
[2] T. Pohl, T. Pattard, and J. M. Rost, Phys. Rev. Lett. **92**, 155003 (2004).
[3] F. Robicheaux and J. D. Hanson, Phys. Rev. Lett. **88**, 055002 (2002).
[4] S. Aloïse, P. OKeeffe, D. Cubaynes, M. Meyer, and A. N. Grum-Grzhimailo, Phys. Rev. Lett. **94**, 223002 (2005).
[5] I. H. Suzuki and N. Saito, J. Electron Spectrosc. Relat. Phenom. **129**, 71 (2003).
[6] J. A. R. Samson and W. C. Stolte, J. Electron Spectrosc. Relat. Phenom. **123**, 265 (2002).
[7] A. A. Sorokin, L. A. Shmaenok, S. V. Bobashev, B. Möbus, and G. Ulm, Phys. Rev. A **58**, 2900 (1998).
[8] I. D. Petrov, V. L. Sukhorukov, E. Leber, and H. Hotop, Eur. Phys. J. D **10**, 53 (2000).
[9] R. Kau, I. D. Petrov, V. L. Sukhorukov, and H. Hotop, J. Phys. B **29**, 5673 (1996).
[10] J. Ganz, B. Lewandowski, A. Siegel, W. Bussert, H. Waibel, M.-W. Ruf, and H. Hotop, J. Phys. B **15**, L485 (1982).

[11] A. Siegel, J. Ganz, W. Bussert, and H. Hotop, J. Phys. B **16**, 2945 (1983).
[12] J. Ganz, M. Raab, H. Hotop, and J. Geiger, Phys. Rev. Lett. **53**, 1547 (1984).
[13] D. Klar, K. Ueda, J. Ganz, K. Harth, W. Bussert, S. Baier, J. M. Weber, M.-W. Ruf, and H. Hotop, J. Phys. B **27**, 4897 (1994).
[14] I. D. Petrov, V. L. Sukhorukov, and H. Hotop, J. Phys. B **32**, 973 (1999).
[15] I. D. Petrov, V. L. Sukhorukov, and H. Hotop, J. Phys. B **35**, 323 (2002).
[16] T. P. Dinneen, C. D. Wallace, K.-Y. N. Tan, and P. L. Gould, Opt. Lett. **17**, 1706 (1992).
[17] J. R. Lowell, T. Northup, B. M. Patterson, T. Takekoshi, and R. J. Knize, Phys. Rev. A **66**, 062704 (2002).
[18] D. N. Madsen and J. W. Thomsen, J. Phys. B **35**, 2173 (2002).
[19] C. Gabbanini, S. Gozzini, and A. Lucchesini, Opt. Commun. **141**, 25 (1997).
[20] J. G. C. Tempelaars, R. J. W. Stas, P. G. M. Sebel, H. C. W. Beijerinck, and E. J. D. Vredenbregt, Eur. Phys. J. D **18**, 113 (2002).
[21] S. J. M. Kuppens, J. G. C. Tempelaars, V. P. Mogendorff, B. J. Claessens, H. C. W. Beijerinck, and E. J. D. Vredenbregt, Phys. Rev. A **65**, 023410 (2002).
[22] J. Javanainen, J. Opt. Soc. Am. B **10**, 572 (1993).
[23] C. G. Townsend, N. H. Edwards, C. J. Cooper, K. P. Zetie, C. J. Foot, A. M. Steane, P. Szriftgiser, H. Perrin, and J. Dalibard, Phys. Rev. A **52**, 1423 (1995).
[24] C. Duzy and H. A. Hyman, Phys. Rev. A **22**, 1878 (1980).
[25] T. N. Chang, J. Phys. B **15**, L81 (1982).
[26] T. N. Chang and Y. S. Kim, Phys. Rev. A **26**, 2728 (1982).